Single Ventricle and Fontan Procedures

Lucia Flors, Patrick T. Norton, and Klaus D. Hagspiel

Contents

Abstract

Univentricular congenital heart diseases include a range of pathologies that result in a functionally single ventricular chamber. The most common pathologies in this group are tricuspid atresia, pulmonary atresia with an intact ventricular septum, hypoplastic left heart syndrome, and a double-inlet ventricle. Although the only curative therapy for these patients is cardiac transplantation, there are several palliative surgical techniques that divert part or all the systemic venous circulation into the pulmonary arteries bypassing the single ventricular chamber. The modern Fontan procedure consists in anastomosing both SVC and IVC to the right pulmonary artery; it is nowadays the last step of single ventricle palliation.

The importance of imaging in these pathologies lies not only in the understanding of the new circuit established after surgical correction, but also in the early detection of the wide spectrum of cardiac and extracardiac complications that can happen due to the new physiological condition. Due to the increased survival of these patients, long-term complications are becoming more common. Imaging patients with single ventricle physiology and particularly following single ventricle palliative procedures is challenging due to the altered anatomy and hemodynamics. While MRI and MRA should be considered the modality of choice due to the inherent lack of

Electronic Supplementary Material The online version of this chapter (doi:10.1007/174_2017_109) contains supplementary material, which is available to authorized users.

L. Flors, M.D., Ph.D. (✉)
Department of Radiology and Medical Imaging, University of Virginia Health System, 1215 Lee St., Charlottesville, VA 22908, USA

Department of Radiology, University of Missouri Health System, MO, USA

P.T. Norton, M.D. • K.D. Hagspiel, M.D.
Department of Radiology and Medical Imaging, University of Virginia Health System, 1215 Lee St., Charlottesville, VA 22908, USA
e-mail: lff8p@virginia.edu

Med Radiol Diagn Imaging (2017)
DOI 10.1007/174_2017_109, © Springer International Publishing AG
Published Online: 01 September 2017

ionizing radiation in this patient population, CT angiography is an important alternative noninvasive imaging technique. In this chapter, we review the different palliative surgical techniques in patients with univentricular heart diseases, and we describe the optimal imaging protocol and the expected surgical anatomy as well as the long-term complications.

Keywords

Fontan procedure • Hypoplastic left heart syndrome • Tricuspid atresia • Pulmonary atresia • Magnetic resonance imaging • Computed tomography

1 Introduction

Some congenital heart diseases show impairment of the normal biventricular physiology. In normal circumstances, pulmonary and systemic circulations are separated and driven by their respective ventricular "pump," but there are several congenital heart diseases, such as hypoplastic left heart syndrome (HLHS), tricuspid atresia, or pulmonary atresia, characterized by having a functional single ventricular chamber (Fredenburg et al. 2011; Khanna et al. 2012; Lu et al. 2012). Physiologically, the single ventricle receives the flow from both pulmonary and systemic circulations with subsequent volume overload and long-term dysfunction.

Although the definitive treatment of these patients is cardiac transplantation, there are several palliative surgical techniques that prevent ventricular volume overload diverting part or all the systemic venous circulation into the pulmonary arteries, and therefore bypassing the single ventricular chamber (Fredenburg et al. 2011; Khanna et al. 2012). The result obtained is a single ventricle that functions both as suction and expelling pump.

The dramatic advances in congenital heart surgery and intensive care medicine have substantially increased the life expectancy of these patients and late complications of the failing Fontan physiology are therefore observed more commonly (Khanna et al. 2012).

Imaging follow-up is essential for anatomical and functional assessment before and after surgery, and early detection of cardiac and extracardiac complications (Lu et al. 2012).

The objective of this chapter is to review the different surgical options in patients with functionally univentricular heart, to describe the optimal imaging protocol, to illustrate the expected normal postsurgical anatomy, and to describe the potential (long-term) complications of these procedures and the spectrum of their imaging findings.

2 Surgical Techniques and Normal Postsurgical Anatomy

The goal of palliative therapy in the setting of heart disease with a functioning single ventricle is to unload the ventricular burden imposed by the pulmonary and systemic circuits flowing in parallel to a system in which they operate in series. This is achieved by removing the subpulmonic pump in lieu of passive systemic venous flow directly into the lungs, thus freeing the single ventricle for pumping oxygenated blood systemically. In the 1940s, it was shown that the right ventricle could be excluded from the pulmonary circuit while maintaining adequate pulmonary blood flow (Rodbard and Wagner 1949). Fontan capitalized on this in 1968 when he performed his landmark surgery for tricuspid atresia, by anastomosing the right atrial appendage directly and the pulmonary artery (Fontan and Baudet 1971). Subsequently, this procedure was modified and adapted to other variants of univentricular hearts.

Fontan circulation can be achieved by either anastomosing the vena cava to the pulmonary artery, with the use of baffles or conduits, or connecting the right atrium to the pulmonary artery after excluding tricuspid flow and repairing any atrial septal defect (classic atriopulmonary connection, classic Fontan) (Fig. 1). However, many patients will require a staged approach rather than primary creation of the Fontan circuit due to unfavorable anatomy and physiology. A staged

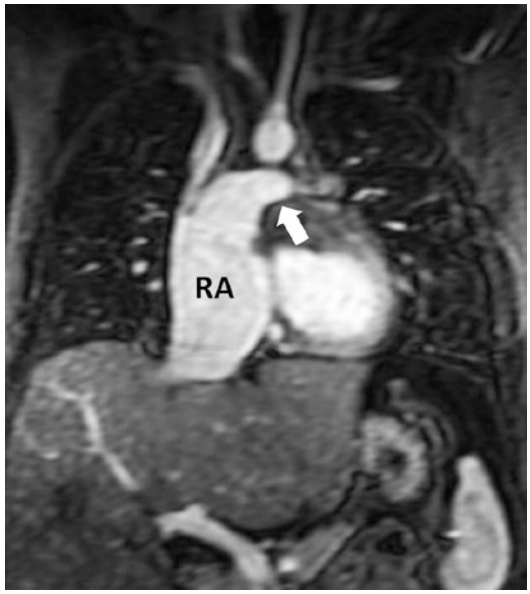

Fig. 1 Classic Fontan procedure for tricuspid atresia correction. Contrast-enhanced MRA image shows the connection between the *right atrium* (RA) and the *right pulmonary artery* (*arrow*). Note the mild dilatation of the RA

Fig. 2 Norwood-Sano procedure for correction of hypoplastic *left heart syndrome* in the neonatal period. Sano conduit seen from the *right ventricle* to the pulmonary artery (*arrow*). Neoaorta created from the amalgamation of the transected MPA with the ascending aorta after the Norwood procedure is also seen (*arrowheads*)

approach allows for appropriate growth of the pulmonary arteries and minimizes acute changes in end-diastolic filling, resulting in a decrease in mortality as compared to a primary Fontan creation (Norwood and Jacobs 1993).

The first stage of palliation of the single ventricle is performed in the neonatal period and consists of controlling pulmonary blood flow, by means of a direct systemic-to-pulmonary artery shunt or pulmonary artery banding; relieving any systemic outflow obstruction; and addressing issues with pulmonary venous return. In cases of HLHS, a Norwood procedure is performed whereby the main pulmonary artery (MPA) is transected and a "neoaorta" is created from the amalgamation of the MPA with the ascending aorta. In combination with aortic arch augmentation, unobstructed systemic flow for aortic growth and coronary perfusion is provided. Pulmonary blood flow (PBF) is regulated via a size-specific conduit from the subclavian or brachiocephalic artery to the pulmonary artery (modified Blalock Taussig shunt) or via a conduit from the right ventricle to the pulmonary artery (Sano shunt) (Fig. 2).

The location of the Blalock Taussig shunt downstream of the neoaortic valve results in continuous PBF in both systole and diastole, creating a situation where retrograde flow could occur in the coronary arteries during diastole. The Sano shunt eliminates the potential for coronary steal, but may lead to decreased ventricular function and increased arrhythmias secondary to the ventriculotomy. However, there is no clear evidence to support superiority of one technique over the other (Ohye et al. 2016).

The second stage of palliation is the creation of a superior cavopulmonary connection, typically occurring at 4–9 months of age, after the pulmonary vasculature has matured. The superior vena cava venous return is directed into the pulmonary arteries, sources of systemic-to-pulmonary arterial blood flow are disconnected or interrupted (e.g., Blalock Taussig shunt, Sano shunt, flow through a stenotic pulmonary valve), and any pulmonary bands are removed. Cardiac output is directed solely to the systemic circulation, reducing the volume work of the heart. The procedure chosen at this stage determines the final technique employed for Fontan completion.

The bidirectional Glenn procedure (BDG) is created by dividing the superior vena cava (SVC) at the SVC-atrial junction, oversewing the atrial

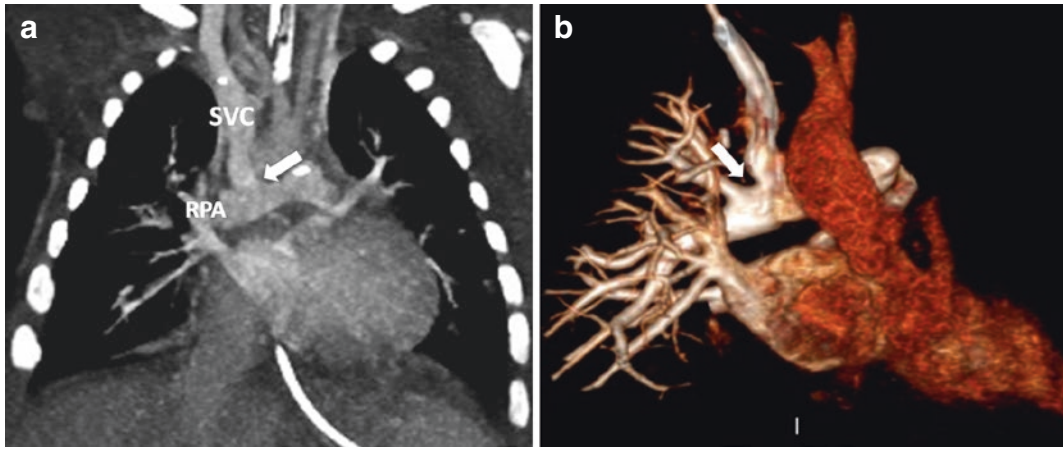

Fig. 3 6-month-old boy with the history of tricuspid atresia status post-bidirectional Glenn. Coronal CT angiography, maximum intensity projection (**a**), and volume rendering 3D (**b**) images show connection (*arrow*) of the superior vena cava (SVC) to the *right pulmonary artery* (RPA)

end, and anastomosing the SVC to the ipsilateral pulmonary artery in an end-to-side fashion (Fig. 3). Continuity of the left and right pulmonary arteries permits blood flow to both lungs. In cases of bilateral SVCs, this anastomosis is performed bilaterally to direct all venous return from the head and upper extremities to the pulmonary arteries. The BDG typically results in a pulmonary-to-systemic blood flow ratio (Qp/Qs) of 0.6:1. BDG is relatively simple as compared to hemi-Fontan procedure (HF), requiring shorter cardiopulmonary bypass time without aortic cross clamping or circulatory arrest. BDG does not address problems with pulmonary artery distortion or stenosis and due to the need for extensive dissection to free the SVC there is an increased risk for phrenic nerve injury (Talwar et al. 2014). In the setting of a BDG, Fontan completion is performed with an extracardiac conduit.

An alternative cavopulmonary connection is the hemi-Fontan procedure (HF), which addresses problems of pulmonary artery anatomy and simplifies lateral tunnel completion of the Fontan. In this procedure, the SVC and pulmonary arteries maintain their anterior-posterior relationship. The SVC is opened along the medial aspect at the atrial junction and amalgamated with the anterior aspect of the pulmonary arteries, using a homograft patch. The pulmonary arteries are augmented with a patch extending from just medial of the right upper lobe branch to the left lobar branch. A homograft patch is also used to create a dam between the right atrium and SVC, directing the superior caval flow into the pulmonary arteries, which can be easily removed at the time of lateral tunnel creation (Spray 2013). Percutaneous completion of the Fontan can be performed by perforation of the dam and stenting from the IVC to the pulmonary artery (Talwar et al. 2014). Additionally, the anteroposterior offset between the caval and pulmonary arterial flow may have some hemodynamic benefit (Bove et al. 2003).

The Fontan completion operation is typically performed at 18–48 months of age. This final stage of single ventricular palliation directs systemic venous return from the inferior vena cava (IVC) into the pulmonary arteries, thereby completing the total cavopulmonary connection. In patients that have undergone HF, a lateral tunnel (LT) is the procedure of choice for completion. The homograft dam is excised and a baffle made of synthetic material is used to isolate flow from the IVC into the pulmonary artery along the lateral aspect of the atrium. The baffle is created so as not to obstruct the atrial septal defect. A fenestration, or hole, is often made in the baffle to maintain cardiac output in high-risk patients. This fenestration maintains

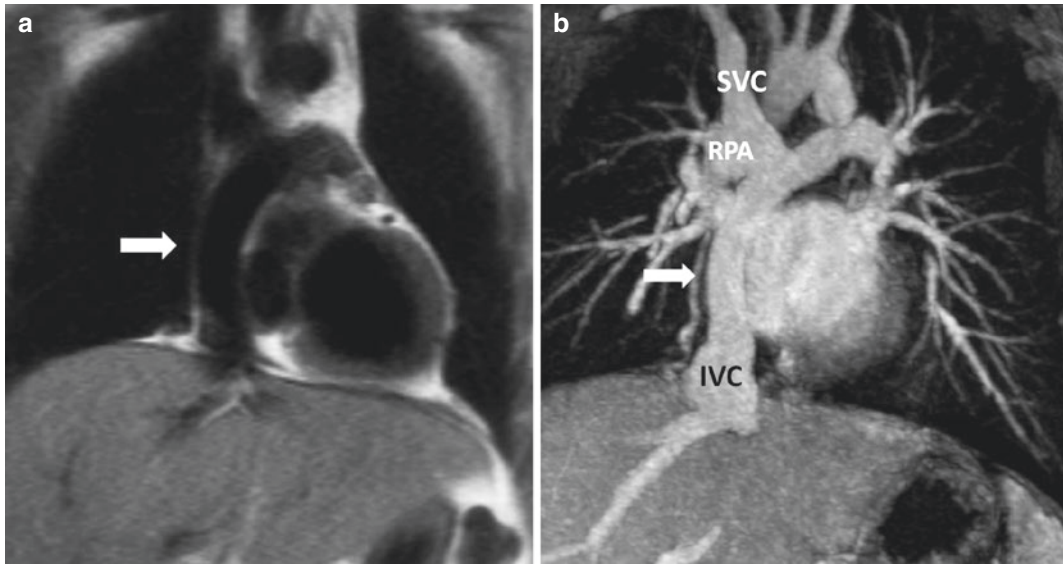

Fig. 4 Fontan procedure for repair of tricuspid atresia. Coronal dark blood spin-echo image (**a**) and contrast-enhanced MRA (**b**) show the total cavopulmonary connection with anastomosis of both the SVC and IVC to the RPA, the latter by means of an extracardiac conduit in this case (*arrow*). An intracardiac lateral tunnel can also be performed

blood flow to the systemic ventricle in the setting of high pulmonary vascular resistance and has the added benefit of reducing the length of postoperative pleural effusions (Bridges et al. 1992).

An extracardiac conduit (ECC) completes the Fontan circuit in the setting of a prior BDG by connecting the IVC above the hepatic veins to the right pulmonary artery by means of an extracardiac synthetic tube graft coursing along the free wall of the right atrium (Fig. 4). Akin to the LT, a fenestration is created by sewing a right atriotomy to a hole in the tube graft. Alternatively, a small ringed tube graft can be connected between the ECC and the right atrium (Bradley 2006). Advantages of ECC as compared to LT include application in a variety of anatomic configurations including heterotaxy syndromes, anomalies of systemic and pulmonary venous drainage, and apico-caval juxtaposition. Furthermore the risk for the right atrium to cause arrhythmias is theoretically lower with an ECC by avoiding exposure to pulmonary artery pressures and a significantly reduced suture burden.

3 Imaging Protocol

Imaging patients with single ventricle physiology and particularly following single ventricle palliative procedures is challenging due to the altered anatomy and hemodynamics. Typically, patients are seen biannually by their cardiologists and echocardiography is performed annually. A routine MRI is often performed 10 years after Fontan operation or when clinical findings and echocardiographic results require further investigation (Rychik 2016). MRI is usually preferred over CTA due to the inherent lack of ionizing radiation in this patient population. Nevertheless, CT angiography is an important alternative noninvasive imaging technique. CTA is particularly useful in emergent situations, in unstable patients, in patients where metal coils obscure structures of interest, and in patients in whom MRI is contraindicated. One of the major advances of CT is the speed of acquisition, and, particularly with the use of modern dual-source scanners, the ability to scan pediatric patients without the use of sedation.

Imaging objectives vary and techniques need to be adopted depending on if the study is performed before or after surgical therapy. In postsurgical patients, the stage of surgical palliation has to be taken into account.

3.1 MRI/MRA Protocol

Evaluation of the patient with single ventricle for surgical planning or postsurgical follow-up should provide information about the size, morphology, and function of the cardiac chambers; the pulmonary arteries and veins; as well as the systemic arteries and veins. It should allow assessment of the baffles and conduits as well as complications of the surgical procedures, which are discussed later in this chapter. MRI is uniquely suited for this purpose due to its lack of ionizing radiation. In our institution, a typical exam lasts approximately 45–60 min (Table 1) and begins with anatomical sequences covering the whole chest using steady-state free precession (SSFP) sequences in axial, sagittal, and coronal planes, as well as black blood axial images using a fast spin-echo (FSE) technique. These are followed by cine SSFP breath-hold images with thin slices and without interslice gap, using stacked axial images in addition to the standard horizontal and vertical long-axis and ventricular short-axis images. These sequences allow functional and morphological assessment of the cardiac chambers, their connections, and the presence of septal defects. Multiphase MR angiography (MRA), preferably using a high-resolution (1 mm isotropic) time-resolved sequence, allows identification and sizing of the pulmonary and systemic arterial and venous

Table 1 CMR imaging protocol at the University of Virginia (1.5 T system preferred over 3 T)

Sequence	Planes	Trade name
1. **Localizers**		
2. **Bright blood imaging** (breath-hold, nongated multislice balanced SSFP images of the entire chest)	Axial Coronal Sagittal	GE: FIESTA, Philips: bFFE, Siemens: TrueFISP
3. **Black blood imaging** of the entire chest with single-shot technique	Axial	GE: SSFSE, Philips: single-shot TSE, Siemens: HASTE
4. **Cine MRI**	Stacked axial without gap standard short and long axes Valve plane Outflow tract	GE: FIESTA, Philips: bFFE, Siemens: TrueFISP
5. **3D contrast-enhanced MRA** in arterial and venous phases (preferably a time-resolved technique) with 1 mm isotropic resolution	Coronal or sagittal oblique	GE: TRICKS, Philips: 4D-TRAK, Siemens: TWIST
6. **Velocity-encoded** cine 2D phase-contrast imaging	Depending on clinical question: pulmonary arteries, aorta, baffle, conduit, systemic veins, pulmonary veins	
7. **Late gadolinium enhancement imaging** 10–15 min after contrast is given 2D segmented inversion recovery GRE or SSFP, PSIR for patients with regular heart rhythm and able to hold breath, otherwise single-shot imaging	2-chamber 3-chamber 4-chamber Short axis	

SSFP steady-state free precession; *FIESTA* fast imaging employing steady-state acquisition; *bFFE* balanced fast field echo; *True FISP* fast imaging with steady-state free precession; *SSFSE* single-shot fast spin echo; *TSE* turbo spin echo; *HASTE* half-Fourier acquisition single-shot turbo spin-echo; *MRA* magnetic resonance angiograph; *TRICKS* time-resolved imaging of contrast kinetics; *TRAK* time-resolved angiography using keyhole; *TWIST* time-resolved angiography with stochastic trajectories; *GRE* gradient-recalled echo; *PSIR* phase-sensitive inversion recovery

system as well as their connections with the heart as well as the baffles and conduits. Due to the lack of radiation and the ability to repeat the image acquisition at multiple time points following the contrast injection, contrast-enhanced MRA is an excellent technique to diagnose thromboembolic complications in the pulmonary vasculature, baffles, and conduits, and assess the systemic veins as well as the arterial system. In general, the spatial resolution of MRA is inferior to CTA and the diagnosis of smaller emboli, pulmonary arteriovenous malformations (PAVMs), and systemic–pulmonary veno-venous shunts frequently requires CTA (Lewis et al. 2015). These complications are discussed later in this chapter. Time-resolved MRA can be performed using dilute contrast and has been shown to provide excellent assessment of the flow dynamics and morphology of the pulmonary circulation as well as the pulmonary perfusion status in Fontan patients (Goo et al. 2007). We typically use 0.1 mmol/kg of gadolinium-based contrast and obtain multiple datasets with a temporal resolution of 3 s with 1 mm isotropic resolution for 90 s with a 10 s scan delay (Video 1). In general, standard extracellular MR contrast agents have been shown to give excellent image quality, and we have not been using blood pool agents in this patient population, which have been used anecdotally (Hashemi et al. 2014).

Velocity-encoded (VENC) cine-phase contrast sequences allow measurement of blood flow in the pulmonary arteries, aorta, baffles and conduits, systemic and pulmonary veins, systemic-to-pulmonary collateral flow, as well as assessment of atrioventricular valves (Latus et al. 2016). The aortopulmonary collateral flow can be quantitated using 2D flow measurements of the ascending aorta, the pulmonary veins, the pulmonary arteries, and the inferior and superior vena cava flow using one of these two equations:

1. Sum of flow in all pulmonary veins—(right + left pulmonary artery flow)
2. Ascending aorta flow—(inferior + superior vena cava flow) (Kutty Heart 2016)

The presence and degree of obstruction in baffles and conduits can also be measured using these techniques. Several newer, albeit not widely available MRI techniques provide even more detailed assessment of the hemodynamics of Fontan patients. Hybrid CMR and X-ray-guided angiography (CMR/XMR) allows to more accurately measure pulmonary vascular resistance than standard catheter techniques (Pushparajah et al. 2015). More recently, the use of particle traces derived from time-resolved 3D MR velocity mapping (4D flow MRI) has been shown to allow in vivo quantification of the caval flow distribution to the PAs in patients with Fontan circulation. It could be demonstrated that 83% of the superior vena cava blood flows to the right pulmonary artery whereas 55% of the inferior vena caval blood flows to the left PA (Bachler et al. 2013).

Late gadolinium enhancement (LGE) of the myocardium using a phase-sensitive ECG-triggered breath-hold inversion recovery sequence allows assessment for myocardial fibrosis and infarction. The presence of LGE is common in late heart Fontan survivors and its presence has been shown to be associated with adverse ventricular mechanics and a higher frequency of nonsustained ventricular tachycardia (Rathod et al. 2010). In one retrospective study involving 215 patients who underwent MRI at a median age of 18.3 years and who underwent the Fontan operation at a median age of 3.6 years, LGE was present in 33% (Rathod et al. 2014).

3.2 CTA Protocol

In cases where MRI is not feasible, CTA is an excellent alternative. We consider high-pitch spiral scanning on dual-source CT scanners without gating or triggering optimal for most patients unless coronary artery evaluation is required in which case we resort to prospective or retrospective techniques. Due to the extreme acquisition speed (up to 74 cm/s table motion) the scan times are

extremely short and we routinely scan children of all ages without sedation or anesthesia. Low kV technique results in effective doses of 1 mSv or less for these scans. If dual-source scanners are not available, at least a 64-channel system should be used—with ECG gating. Proper contrast timing is critical and will depend according to what stage of surgical palliation the study is performed in.

After stage 1 palliation, performed in the neonatal period, patients with systemic-to-pulmonary arterial shunts are typically not at risk to develop pulmonary embolism, due to the absent connection of the pulmonary arteries with systemic veins. They do however have a 1–17% risk of shunt thrombosis, which occasionally leads to the need for imaging beyond echocardiography (Ghadimi Mahani et al. 2016). Conduit stenosis also occurs in a small percentage and can necessitate cross-sectional imaging. In these cases, CT pulmonary angiography (CTPA) is best performed during the pulmonary arterial phase. A venous injection into the lower extremities eliminates streak artifacts that would otherwise affect a scan with an upper extremity venous injection, particularly in children where low kV settings are used (Ghadimi Mahani et al. 2016).

For stage 2, blood from the superior vena cava is redirected to the pulmonary arteries, either via a bidirectional Glenn or a hemi-Fontan procedure. In this stage thrombosis and thromboembolic events are infrequent and often caused by catheters in the upper venous system. CTA in this phase is best performed with lower extremity venous access with the scan started after optimal enhancement of the SVC or bilateral jugular veins with contrast monitoring in the neck or mediastinum. The contrast flows at this stage from the IVC to the ventricle to the systemic arteries, and returns from the brain via the jugular veins. Using this technique, homogeneous enhancement of the pulmonary arteries without inflow of nonopacified blood simulating filling defects is usually achieved. In addition, as the scan is acquired during the arterial phase, the diagnosis of systemic-to-pulmonary arterial collaterals is possible.

The prevalence of thrombosis and thromboembolic events is higher after completion of the total cavopulmonary connection (stage 3). CTPA is suitable to diagnose or exclude thromboembolic in these patients with high accuracy, if performed properly. Standard CTPA techniques using single upper extremity venous access suffer from mixing of opacified blood from the SVC and unopacified blood from the IVC resulting in a large number of nondiagnostic or false-positive studies (Sandler et al. 2014). One way to obviate this problem with single upper extremity venous access is to increase the contrast volume and image with a scan delay of 70–80 s. This results in homogeneous enhancement of the pulmonary arteries and allows the diagnosis of PE. Recommended contrast doses are up to 2 mL/kg in smaller children (we usually hand-inject smaller children and aim for duration of injection of 10–15 s; in older children we use power injectors with flow rates between 0.6 and 2 mL/s) and a total dose of 150 mL in adults with a flow rate of 2 mL/s. If simultaneous aortic enhancement is also desired, the flow rate can be increased to 3–5 mL/s toward the end of the study. A timing bolus or bolus tracking technique is used to determine the time from injection to aortic peak (Ghadimi Mahani et al. 2016). It has to be noted that all intravenous injections in these patients need to be absolutely free of air due to the frequent presence of fenestrations which represent right to left shunts and put the patient at risk of stroke from air emboli.

The optimal technique requires dual venous access, typically one in an antecubital vein and the other in a dorsal foot vein. Alternatively, femoral access can be chosen in adults. Contrast is injected with two power injectors if available with 60% of contrast injected into the lower extremity. Recommended contrast dose is up to 2 mL/kg of 370 mg iodine/mL or up to 3 mL/kg of 300 mg iodine/mL contrast agent. Recommended flow rates are 2–2.5 mL/s in the upper extremity and 3–4 mL/s in the lower extremity. Contrast injection should be followed by a saline flush. A monitoring scan is performed at the level of the carina. The scan is

initiated when the contrast arrives in the left pulmonary artery, which typically occurs after the right PA (Ghadimi Mahani et al. 2016). The dual venous access is also recommended in the ACR–NASCI–SIR–SPR Practice Parameters for the performance of CTA (2016). A 60–90 s delayed scan can be performed in addition depending on the clinical question.

4 Complications

Late complications arising from the new hemodynamic and physiological conditions are observed with increasing frequency due to prolonged survival of these patients. Currently, survival rates are around 85% at 20 years (Khanna et al. 2012).

High pulmonary vascular resistance, anatomical alterations in the pulmonary arteries, increased systemic venous pressure, and ventricular dysfunction are some risk factors that predict a worse outcome and more frequent occurrence of complications (Fredenburg et al. 2011); these can be categorized as cardiac or extracardiac.

4.1 Cardiac Complications

The most common cardiac complication after the classic Fontan technique is atrial enlargement (Fig. 5), which predisposes to arrhythmias and thromboembolic events (Fredenburg et al. 2011; Khanna et al. 2012; de Leval 1998; Soler et al. 2007). Pulmonary embolism secondary to atrial thrombus is the most common cause of out-of-hospital death in patients who have undergone a Fontan procedure (Gewillig 2005). Arrhythmias can also be seen after lateral tunnel total cavopulmonary connection and be the result of atrial suture load and injury to the sinoatrial node during atriotomy (Lewis et al. 2015). When ablation is required, imaging planning is usually helpful.

Ventricular dysfunction is common in longstanding Fontan circuits, usually as a result of chronically elevated afterload and reduced preload. Ventricular dilatation, hypertrophy, and dysfunction can be assessed by imaging.

Atrioventricular valve regurgitation, leak, stenosis (Fig. 6), or thrombosis (Fig. 7) of the conduit are additional potential complications of modern Fontan procedure (Fredenburg et al. 2011;

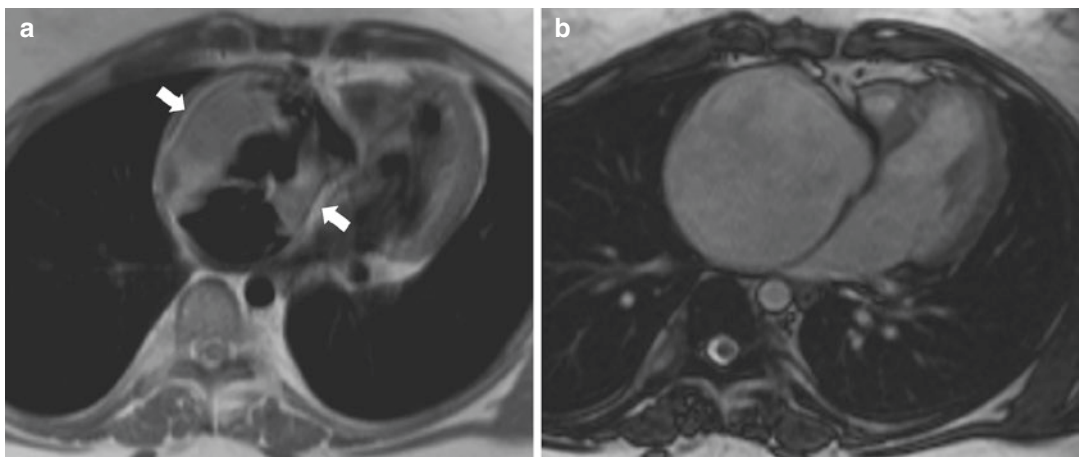

Fig. 5 29-year-old female status post-classic Fontan for tricuspid atresia repair. Dark blood spin-echo (**a**) and bright blood gradient-echo SSFP (**b**) images show severe *right atrial enlargement*. Artifact secondary to slow flow within the dilated atrium (*arrows*) may mimic thrombosis on dark blood imaging (**a**). Patent *right atrium* without evidence of thrombosis was seen on SSFP (**b**) and contrast-enhanced MRA (not shown)

Khanna et al. 2012; de Leval 1998; Soler et al. 2007). Differentiating thrombus from slow-flow artifact may be sometimes challenging (Fig. 5). As described before, optimal contrast timing is paramount to assess conduit thrombosis especially when CTA is performed.

Fig. 6 Fontan procedure for repair of tricuspid atresia. Coronal contrast-enhanced MRA shows mild focal stenosis of the extracardiac Fontan conduit (*arrow*)

4.2 Extracardiac Complications

There is a wide range of extracardiac complications occurring in these patients and imaging plays an important role in the early diagnosis. These can be broadly categorized into complications involving the pulmonary arteries, conditions entailing right-to-left or left-to-right shunting, and hepatic and lymphatic complications.

4.2.1 Pulmonary Arteries

The low pressures achieved after the Fontan repair paradoxically condition an increase in the pulmonary vascular resistance (Fredenburg et al. 2011). This complication is attributed to the absence of pulsatility of the pulmonary arteries, the inability to achieve complete filling of the pulmonary vasculature, and the increase of pulmonary lymphatic pressure (Fredenburg et al. 2011; de Leval 1998). Pulmonary vascular resistance is a determinant factor in the cardiac output of this new hemodynamic condition.

Pulmonary vascular resistance may also be affected by morphological alterations in the pulmonary arteries, mainly stenosis, which frequently occur at the site of anastomosis (Fredenburg et al. 2011). Stenosis of the left pulmonary artery by extrinsic compression of an enlarged aortic root can also be seen; this is

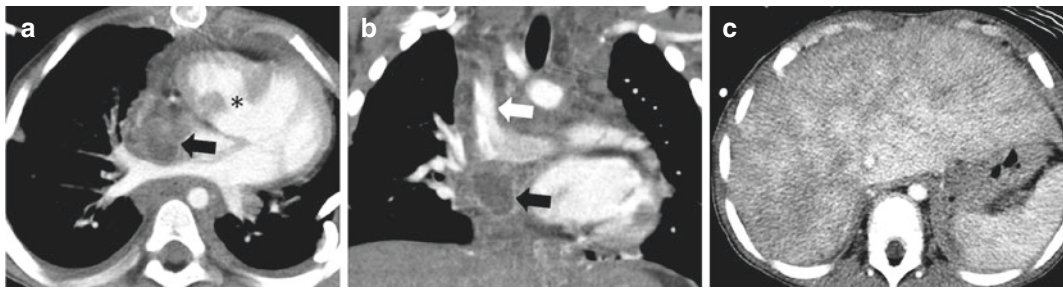

Fig. 7 3-year-old male with recent Fontan procedure for double-outlet *right ventricular repair* and acute thrombosis of the Fontan conduit. Axial (**a**) and coronal (**b**) CTA images show a heterogeneous peripherally enhancing filling defect within the extracardiac inferior vena cava to pulmonary artery shunt (*black arrow*). The superior vena cava has been routed into the *right pulmonary artery* (*white arrow*). A large VSD (*asterisk*) and small *right ventricular chamber* can also be seen on **a**. Hepatic venous congestion is seen on the *upper abdomen* (**c**)

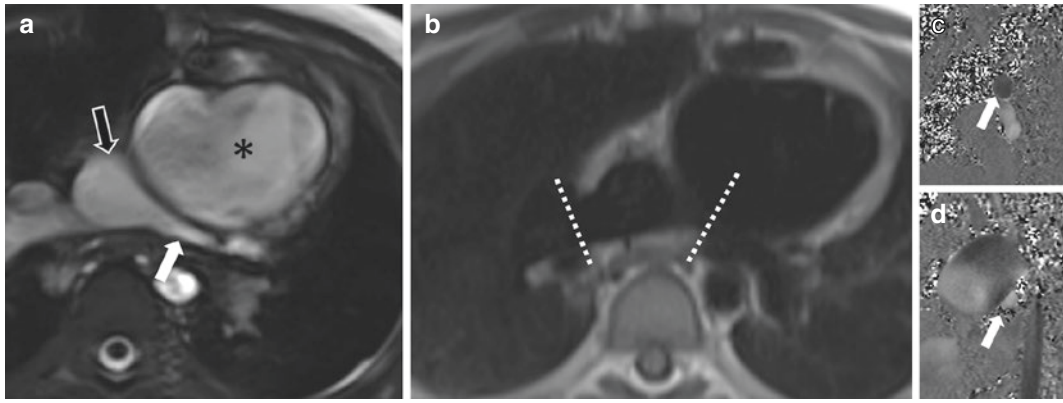

Fig. 8 10-year-old male with the history of hypoplastic *left heart syndrome* status post-staged extracardiac fenestrated Fontan and prior Norwood procedure. Bright blood axial SSFP image (**a**) shows the Fontan conduit (*black arrow*) connecting to the pulmonary arteries. The *left pulmonary artery* is small in size (*white arrow*) with evidence of compression from a severely dilated neo-ascending aorta (*asterisk*). The *right pulmonary artery* is of normal size. Differential pulmonary blood flow calculated using velocity-encoded phase-contrast (VENC) imaging obtained perpendicular to the pulmonary arteries following the plane marked by the dashed lines on the dark blood axial image (**b**), through the *right* (**c**) and *left* (**d**) pulmonary arteries (*arrows*), revealed asymmetric pulmonary flow, 80% of a total flow to the *right* and 20% of total flow to the *left*

particularly common in cases of hypoplastic left ventricle that underwent Fontan palliation and prior Norwood connection (aorta and pulmonary artery connection) due to compression by a dilated neoaorta (Fig. 8) (Lewis et al. 2015). Early detection and treatment of pulmonary artery stenosis can improve system functionality. Stents are often placed in the pulmonary arteries to maintain patency. Due to metallic artifact, these are usually better assessed with CTA.

After completion of the total cavopulmonary connection the prevalence of thrombosis and thromboembolic events has been found to range from 1 to 33%, with the highest risk immediately postsurgery and then again late (10 + years) following the surgery (McCrindle et al. 2013).

4.2.2 Shunting

Right-to-left shunts may occur due to the development of pulmonary arteriovenous fistulae (PAVFs) and the formation of systemic-pulmonary venovenous shunts (VVS) (Fredenburg et al. 2011; Khanna et al. 2012; de Leval 1998) which usually cause desaturation and cyanosis (Khanna et al. 2012).

The lack of pulsatility in the pulmonary arteries and the absence or asymmetrical distribution of the hepatoenteric inflow in the lungs are considered potential etiological factors (Khanna et al. 2012; Ashrafian and Swan 2002; Srivastava et al. 1995) but the exact etiology of PAVF is not clearly known. Some authors attribute the PAVF formation to an unknown "hepatic factor." They hypothesized that the liver may be responsible for the degradation of a vasodilating substance (Duncan and Desai 2003; Kim et al. 2009), and may also be the source of vasoactive substances that function as inhibitors of pulmonary vascular dilatation or recruitment (Duncan and Desai 2003). In fact, an increased risk of occurrence of these malformations in lungs with absent hepatoenteric flow during "the Glenn stage" and reversibility of this condition after the Fontan completion has been seen (Lu et al. 2012).

Venovenous collateral development with connection between the systemic and pulmonary circulation, systemic-pulmonary VVS, is a consequence of the existence of an elevated central venous pressure (Khanna et al. 2012; Ashrafian and Swan 2002; Srivastava et al. 1995). These anomalous vessels are seen in the mediastinum connecting the subclavian veins, the inferior or inferior vena cava, and the hepatic veins with the pulmonary veins.

Maximal intensity projection (MIP) reconstructions can help identifying PAVF and VVs on CTA images (2) (Fig. 9). When clusters of small innumerable PAVFs occur, multifocal ground-glass opacities can be seen on CT (Fig. 10); additional regional early venous drainage is also frequently seen (Figs. 9 and 10). MRI has become an excellent and accurate noninvasive method for quantifying functional parameters, such as pulmonary and systemic flow, and right-to-left shunting resulting from collateral flow and fistulae (Whitehead et al. 2009; Grosse-Wortmann et al. 2009). Excellent hemodynamic assessment of the PAVFs can also be obtained with time-resolved MRA (Fig. 10).

Left-to-right shunting can also occur via major aortopulmonary collaterals, which can arise from the thoracic aorta, and brachiocephalic and internal mammary arteries. Other potential causes of shunting include surgical fenestrations and residual atrial septal defects.

4.2.3 Hepatic Complications

Elevated systemic venous pressure after a Fontan procedure causes chronic passive venous congestion that has negative effects on the liver parenchyma. The increased retrograde pressure in the hepatic sinusoids may ultimately lead to centrilobular, necrosis, sinusoidal fibrosis, cirrhosis, and portal hypertension (Fredenburg et al. 2011; Khanna et al. 2012; Ghaferi and Hutchins 2005). In addition to hepatic vein-centered liver fibrosis, portal-based fibrosis has been demonstrated recently in the majority of patients who died soon after the Fontan procedure, which suggests a multifactorial origin of the disease (Schwartz et al. 2012).

As occurs in all other causes of cirrhosis, patients with cardiac cirrhosis may develop dysplastic nodules and hepatocellular carcinomas

Fig. 9 20-year-old female with multiple PAVF and VVS presented with cyanosis and oxygen saturation of 82%. Contrast-enhanced CT images (MIP reconstructions) show strong and early contrast opacification of the *right upper pulmonary artery* (PA) and *right upper pulmonary vein* (PV) due to the presence of innumerable PAVFs in the *right upper lobe*. Collateral circulation is also seen within the mediastinum (*arrow*) representing several systemic-pulmonary VVS that connect the *left subclavian vein* and the SVC with the pulmonary veins (*black arrow*). *PAVF* pulmonary arteriovenous fistulae; *VVS* venovenous shunts

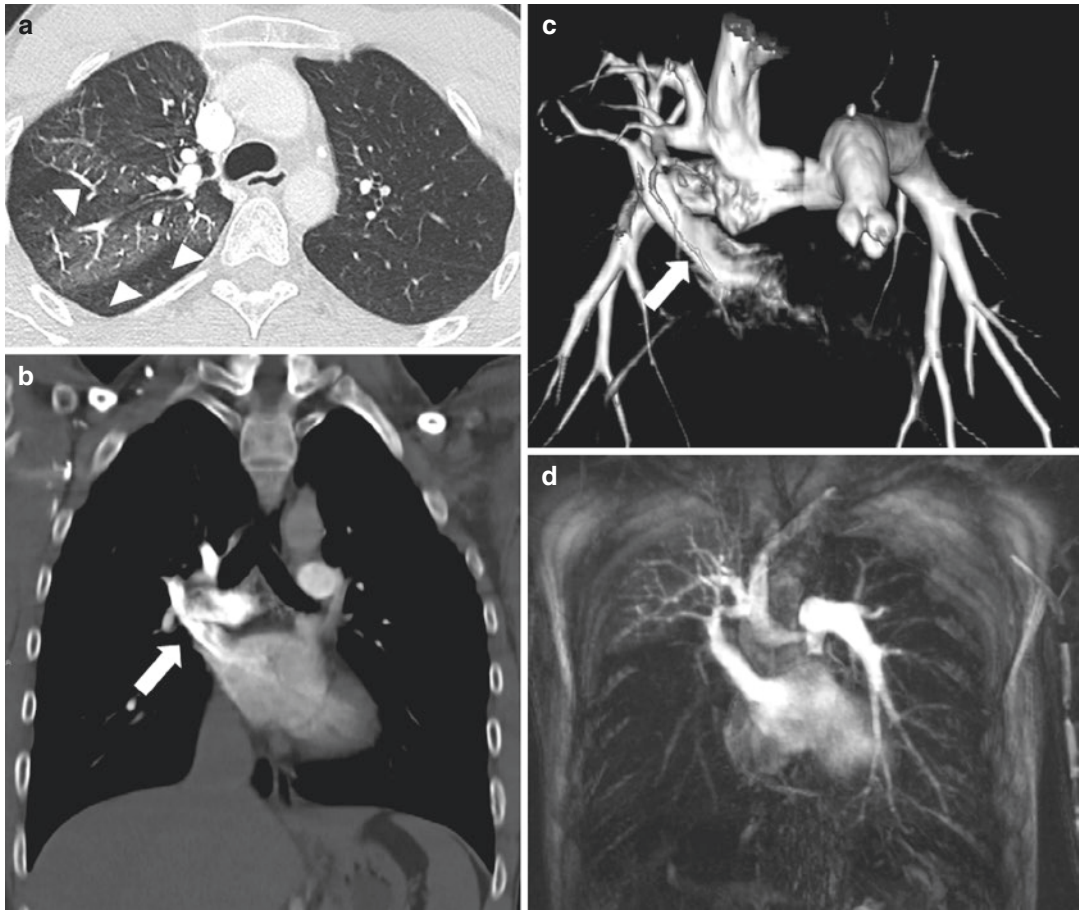

Fig. 10 13-year-old girl with Fontan procedure for pulmonary atresia correction presented with shortness of breath. Contrast-enhanced thoracic CT image shows countless small PAVFs in the RUL presenting as ground-glass opacities (*arrowheads*) (**a**). Strong and early contrast opacification of the *right upper pulmonary vein* (*white arrow*) is seen in the MIP (**b**) and volume-rendering (**c**) reconstructions due to the presence of the PAVFs. Time-resolved contrast-enhanced MRA (**d**) allows excellent assessment of the hemodynamics of the PAVFs

(HCC) (Ghaferi and Hutchins 2005; Asrani et al. 2013). In addition to the alpha-fetoprotein level, imaging surveillance is, therefore, recommended (Ghaferi and Hutchins 2005). Some authors advocate the use of CT and ultrasound, considering MRI and target biopsy for large and enlarging nodules (Kiesewetter et al. 2007).

In the first stage of passive hepatic congestion a typical reticular enhancement pattern in the portal phase, more pronounced in the periphery, is seen (Khanna et al. 2012) (Figs. 7 and 11). Chronic increase of the venous pressure results in the development of regenerative nodules and the formation of intra- and extrahepatic VVS (Khanna et al. 2012; Ghaferi and Hutchins 2005; Kiesewetter et al. 2007; Bryant et al. 2011). Regenerative nodules have a similar appearance to focal nodular hyperplasia (FNH) on dynamic contrast-enhanced imaging—both are brightly hyperenhancing lesions on arterial phase and slightly hyperintense or isointense to the background liver on the venous phase—and must be differentiated from HCC which shows the typical contrast washout on delayed images (2) among other distinctive features. Benign hypervascular hepatic nodules, frequently located in the periphery, are common in the failing Fontan circulation. A recent study showed that postmortem histology

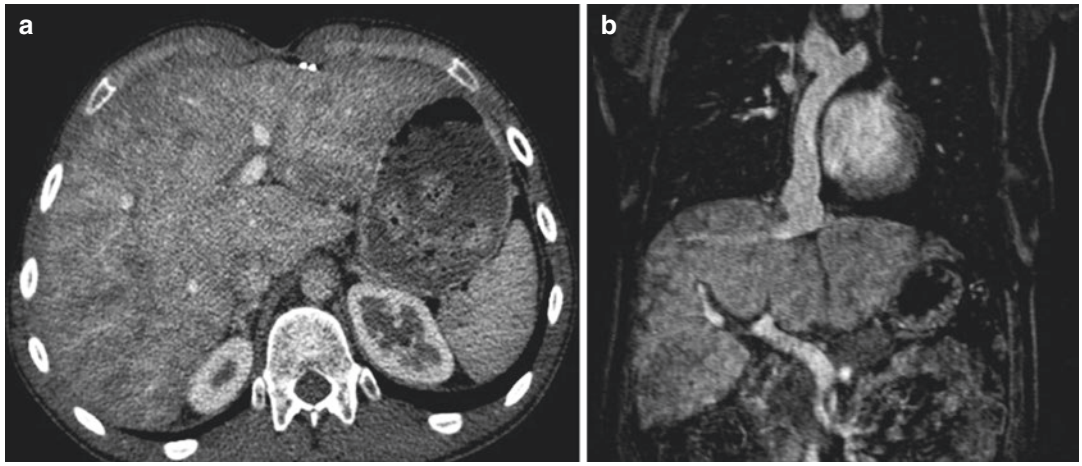

Fig. 11 Hepatic venous congestion after Fontan procedure in two different patients. CT image (**a**) and portal-phase contrast-enhanced MRI (**b**) images show heterogeneity and peripheral perfusion alteration. Extracardiac Fontan conduit is also seen (*arrow*)

suggests that FNH is the underlying pathology and their presence very likely indicates arterialization of hepatic blood flow and reciprocal portal venous deprivation (Bryant et al. 2011).

4.2.4 Lymphatic Complications

In the lungs, the elevated systemic venous pressure and secondary increased lymphatic pressure can cause interstitial pulmonary edema, and pleural and pericardial effusion (de Leval 1998). Plastic bronchitis is another rare potential complication of lymphatic dysfunction (Fredenburg et al. 2011; Goo et al. 2008). Patients usually present with cough and expectoration. Impaired lymphatic drainage and low cardiac output cause hypersecretion of mucin and formation of large and dense secretions that impact into the airway (Khanna et al. 2012). CT findings usually include bronchial wall thickening, mucous plugging, and atelectasis.

Protein-losing enteropathy and ascites are the most relevant abdominal complications derived from the increased lymphatic pressure. Protein-losing enteropathy is a late, serious complication with a poor prognosis (Fredenburg et al. 2011; Khanna et al. 2012; de Leval 1998; Feldt et al. 1996), thought to be associated with the venous and lymphatic congestion that occurs in the splanchnic circuit causing protein loss into the intestinal lumen

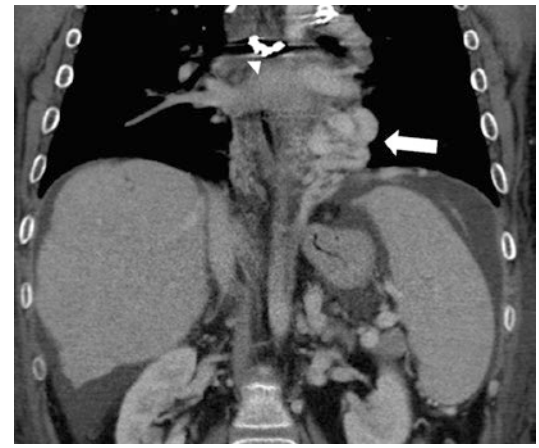

Fig. 12 16-year-old male patient with cardiac cirrhosis, portal hypertension, and protein-losing enteropathy after Fontan procedure. Coronal abdominal CT images show morphologic changes of cirrhosis and portal hypertension with ascites and splenomegaly. Large systemic-pulmonary venovenous shunts (VVS) from the *left suprahepatic vein* to the *left inferior pulmonary vein* are also seen (*arrow*). Coils from prior embolization of VVS also noted in the mediastinum (*arrowhead*)

with the subsequent hypoalbuminemia and immunodeficiency (Fredenburg et al. 2011; Khanna et al. 2012). The hypoproteinemia may also be the cause of pleural effusion and ascites. MRI and CT are rarely helpful in the diagnoses of this condition. Ascites (Fig. 12) and bowel wall thickening are the nonspecific findings usually seen.

Conclusion

The Fontan procedure is a palliative surgical therapy indicated for patients with a variety of congenital cardiac diseases which results in univentricular physiology. Although many modifications to the original description have been employed, the main objective of this technique is based on connecting the systemic venous flow to the pulmonary circulation in order to avoid overloading the single ventricular chamber. Because of its comprehensive assessment, CMR has become the best imaging technique in the postoperative evaluation of these patients. In cases where MRI is not feasible CTA is an excellent alternative. Familiarity with the surgical procedure, the new postsurgical anatomy and physiology, and the spectrum of long-term cardiac and extracardiac complications are becoming more important as the survival of these patients increases.

References

Ashrafian H, Swan L (2002) The mechanism of formation of pulmonary arteriovenous malformations associated with the classic Glenn shunt (superior cavopulmonary anastomosis). Heart 88:639

Asrani SK, Warnes CA, Kamath PS (2013) Hepatocellular carcinoma after the Fontan procedure. N Engl J Med 368:1756–1757

Bachler P, Valverde I, Pinochet N et al (2013) Caval blood flow distribution in patients with Fontan circulation: quantification by using particle traces from 4D flow MR imaging. Radiology 267:67–75

Bove EL, de Leval MR, Migliavacca F, Guadagni G, Dubini G (2003) Computational fluid dynamics in the evaluation of hemodynamic performance of cavopulmonary connections after the Norwood procedure for hypoplastic left heart syndrome. J Thorac Cardiovasc Surg 126:1040–1047

Bradley SM (2006) Extracardiac conduit Fontan procedure. Oper Tech Thorac Cardiovasc Surg 11:123–140

Bridges ND, Mayer JE Jr, Lock JE et al (1992) Effect of baffle fenestration on outcome of the modified Fontan operation. Circulation 86:1762–1769

Bryant T, Ahmad Z, Millward-Sadler H et al (2011) Arterialised hepatic nodules in the Fontan circulation: hepatico-cardiac interactions. Int J Cardiol 151:268–272

ACR NASCI SIR SPR practice parameters for the performance and interpretation of body computed tomography angiography (CTA) (2016). Available: https://www.acr.org/~/media/168A72F0C6004CA9A649DBD6EA9368DE.pdf. Accessed 2 Jan 2017

Duncan BW, Desai S (2003) Pulmonary arteriovenous malformations after cavopulmonary anastomosis. Ann Thorac Surg 76:1759–1766

Feldt RH, Driscoll DJ, Offord KP et al (1996) Protein-losing enteropathy after the Fontan operation. J Thorac Cardiovasc Surg 112:672–680

Fontan F, Baudet E (1971) Surgical repair of tricuspid atresia. Thorax 26:240–248

Fredenburg TB, Johnson TR, Cohen MD (2011) The Fontan procedure: anatomy, complications, and manifestations of failure. Radiographics 31:453–463

Gewillig M (2005) The Fontan circulation. Heart 91:839–846

Ghadimi Mahani M, Agarwal PP, Rigsby CK et al (2016) CT for assessment of thrombosis and pulmonary embolism in multiple stages of single-ventricle palliation: challenges and suggested protocols. Radiographics 36:1273–1284

Ghaferi AA, Hutchins GM (2005) Progression of liver pathology in patients undergoing the Fontan procedure: chronic passive congestion, cardiac cirrhosis, hepatic adenoma, and hepatocellular carcinoma. J Thorac Cardiovasc Surg 129:1348–1352

Goo HW, Yang DH, Park IS et al (2007) Time-resolved three-dimensional contrast-enhanced magnetic resonance angiography in patients who have undergone a Fontan operation or bidirectional cavopulmonary connection: initial experience. J Magn Reson Imaging 25:727–736

Goo HW, Jhang WK, Kim YH et al (2008) CT findings of plastic bronchitis in children after a Fontan operation. Pediatr Radiol 38:989–993

Grosse-Wortmann L, Al-Otay A, Yoo SJ (2009) Aortopulmonary collaterals after bidirectional cavopulmonary connection or Fontan completion: quantification with MRI. Circ Cardiovasc Imaging 2:219–225

Hashemi S, Parks WJ, Slesnick TC (2014) 3D inversion recovery gradient echo respiratory navigator imaging using Gadofosveset Trisodium in a Fontan Y-graft patient. Int J Cardiovasc Imaging 30:993–994

Khanna G, Bhalla S, Krishnamurthy R, Canter C (2012) Extracardiac complications of the Fontan circuit. Pediatr Radiol 42:233–241

Kiesewetter CH, Sheron N, Vettukattill JJ et al (2007) Hepatic changes in the failing Fontan circulation. Heart 93:579–584

Kim SJ, Bae EJ, Lee JY, Lim HG, Lee C, Lee CH (2009) Inclusion of hepatic venous drainage in patients with pulmonary arteriovenous fistulas. Ann Thorac Surg 87:548–553

Latus H, Gerstner B, Kerst G et al (2016) Effect of inhaled nitric oxide on blood flow dynamics in patients after the Fontan procedure using cardiovascular magnetic resonance flow measurements. Pediatr Cardiol 37:504–511

de Leval MR (1998) The Fontan circulation: what have we learned? What to expect? Pediatr Cardiol 19:316–320

Lewis G, Thorne S, Clift P, Holloway B (2015) Cross-sectional imaging of the Fontan circuit in adult congenital heart disease. Clin Radiol 70:667–675

Lu JC, Dorfman AL, Attili AK, Ghadimi Mahani M, Dillman JR, Agarwal PP (2012) Evaluation with cardiovascular MR imaging of baffles and conduits used in palliation or repair of congenital heart disease. Radiographics 32:E107–E127

McCrindle BW, Manlhiot C, Cochrane A et al (2013) Factors associated with thrombotic complications after the Fontan procedure: a secondary analysis of a multicenter, randomized trial of primary thromboprophylaxis for 2 years after the Fontan procedure. J Am Coll Cardiol 61:346–353

Norwood WI, Jacobs ML (1993) Fontan's procedure in two stages. Am J Surg 166:548–551

Ohye RG, Schranz D, D'Udekem Y (2016) Current therapy for hypoplastic left heart syndrome and related single ventricle lesions. Circulation 134:1265–1279

Pushparajah K, Tzifa A, Bell A et al (2015) Cardiovascular magnetic resonance catheterization derived pulmonary vascular resistance and medium-term outcomes in congenital heart disease. J Cardiovasc Magn Reson 17:28

Rathod RH, Prakash A, Powell AJ, Geva T (2010) Myocardial fibrosis identified by cardiac magnetic resonance late gadolinium enhancement is associated with adverse ventricular mechanics and ventricular tachycardia late after Fontan operation. J Am Coll Cardiol 55:1721–1728

Rathod RH, Prakash A, Kim YY et al (2014) Cardiac magnetic resonance parameters predict transplantation-free survival in patients with fontan circulation. Circ Cardiovasc Imaging 7:502–509

Rodbard S, Wagner D (1949) By-passing the right ventricle. Proc Soc Exp Biol Med 71:69

Rychik J (2016) The relentless effects of the Fontan paradox. Semin Thorac Cardiovasc Surg Pediatr Card Surg Annu 19:37–43

Sandler KL, Markham LW, Mah ML, Byrum EP, Williams JR (2014) Optimizing CT angiography in patients with Fontan physiology: single-center experience of dual-site power injection. Clin Radiol 69:e562–e567

Schwartz MC, Sullivan L, Cohen MS et al (2012) Hepatic pathology may develop before the Fontan operation in children with functional single ventricle: an autopsy study. J Thorac Cardiovasc Surg 143:904–909

Soler R, Rodriguez E, Alvarez M, Raposo I (2007) Postoperative imaging in cyanotic congenital heart diseases: part 2 complications. AJR Am J Roentgenol 189:1361–1369

Spray TL (2013) Hemi-Fontan procedure. Oper Tech Thorac Cardiovasc Surg 18:124–137

Srivastava D, Preminger T, Lock JE et al (1995) Hepatic venous blood and the development of pulmonary arteriovenous malformations in congenital heart disease. Circulation 92:1217–1222

Talwar S, Nair VV, Choudhary SK, Airan B (2014) The Hemi-Fontan operation: a critical overview. Ann Pediatr Cardiol 7:120–125

Whitehead KK, Gillespie MJ, Harris MA, Fogel MA, Rome JJ (2009) Noninvasive quantification of systemic-to-pulmonary collateral flow: a major source of inefficiency in patients with superior cavopulmonary connections. Circ Cardiovasc Imaging 2:405–411